Condition of Stable Operation in a Hall Thruster

Naoji Yamamoto, Kimiya Komurasaki and Yoshihiro Arakawa
University of Tokyo, Hongo 7-3-1, Bunkyo-ku, Tokyo, 113-8656, Japan
+81-3-5841-6586
naoji@al.t.u-tokyo.ac.jp

IEPC-03-086

Abstract

An oscillation model at frequency range of 10-100kHz in a Hall thruster is proposed where the oscillation is due to ionization interaction between electrons and neutral particles and where the phase velocity of plasma is assumed zero. Oscillation amplitude was measured using a 1kW class Hall thruster to validate this model. The predicted unstable operational condition agreed qualitatively with the experimental results. This model shows that anode configuration will affect stability, and experimental results supported this.

Nomenclature

B	: magnetic flux density
D	: diffusion coefficient
E	: electric field strength
e	: electronic charge
I_d	: discharge current
I_{sp}	: specific impulse
k	: wave number
k_B	: Boltzmann's constant
L	: ionization zone length
M	: particle mass
$\dot{m}$	: mass flow rate
N	: number density
P	: pressure
Q	: particle flow rate
r_L	: Larmor radius
S	: cross-section
T	: temperature
V	: volume
V_e	: electron velocity
V_n	: neutral atom velocity
V_d	: discharge voltage
z	: axial direction
α	: ion loss coefficient
β	: excitation coefficient
γ	: ionization coefficient
Δ	: oscillation amplitude
δ	: secondary electron emission coefficient
ε	: ionization energy
η_a	: acceleration efficiency
η_u	: propellant utilization
λ_{ne}	: neutral-electron mean free path
μ	: mobility
τ	: measurement time
ϕ	: space potential
ω	: oscillation frequency

Subscripts

a	:	anode layer type
e	:	electron
i	:	ion
n	:	neutral atom
w	:	wall
anode	:	anode side
exit	:	exit side

1. Introduction

One of the problems in Hall thrusters is discharge current oscillation, especially at frequency range of 10-100 kHz. Since it cause the operation to cease as well as they bear down on PPU. Understanding the oscillations is essential for future improvement of Hall thruster and PPU design. There have been many studies about these oscillation phenomena, and they revealed that these oscillations would be caused by ionization instability.[1-3] They, however, were not enough to adequately describe this oscillation, especially stability criteria for a certain range of magnetic flux density. The aim of this study is 1) to propose a physical model 2) to validate the model and 3) to depress the oscillation.

2. The Experimental Equipment

Thruster

Figure 1 (a) shows the cross-section of a 1kW class magnetic layer type Hall thruster. The inner and outer diameter of the discharge chamber is 48mm and 62mm, respectively. The wall is made of BN. The anode is located at 21mm upstream end of the acceleration channel. It can be Anode layer type Hall thruster when the wall is changed by two guard rings made of stainless steel, which are kept at cathode potential as shown in Fig. 1 (b). It has a hollow annular anode. The anode width and anode location can be changed. The anode width is variable from 1mm to 3mm and the acceleration length is from 1mm to 4mm. The magnetic flux density is variable by changing the coil current. Figure 2 shows the magnetic field distribution along the chamber median at the coil current of 4A. Magnetic flux density is maximum at the chamber exit and minimum at the anode. Xenon was used as a propellant gas. As an electron source, a filament cathode (ϕ0.27mm×500mm×3, 2% thoriated tungsten) was used, since the hollow cathode in itself can be a noise source as shown in Fig. 3.

Vacuum Chamber

A 2m-diameter by 3m long vacuum chamber was used through the experiments. The pumping system consists of a diffusion pump, a mechanical booster pump and two rotary pumps. The background pressure was maintained under 5.3×10^{-3} Pa for most of the operating conditions.

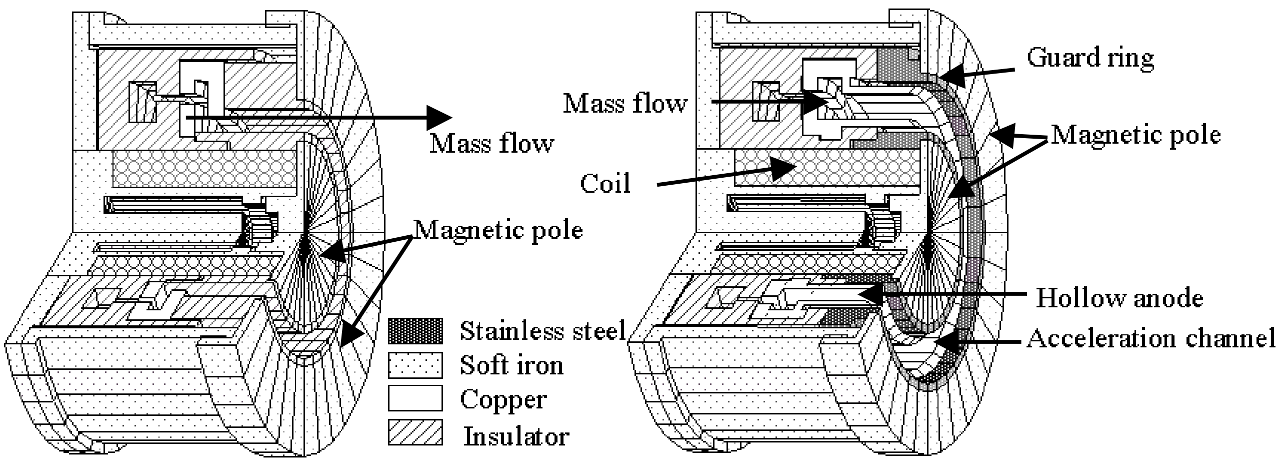

(a)Magnetic layer type (b) Anode layer type

Fig. 1 Cross section of the Hall Thruster developed at University of Tokyo.

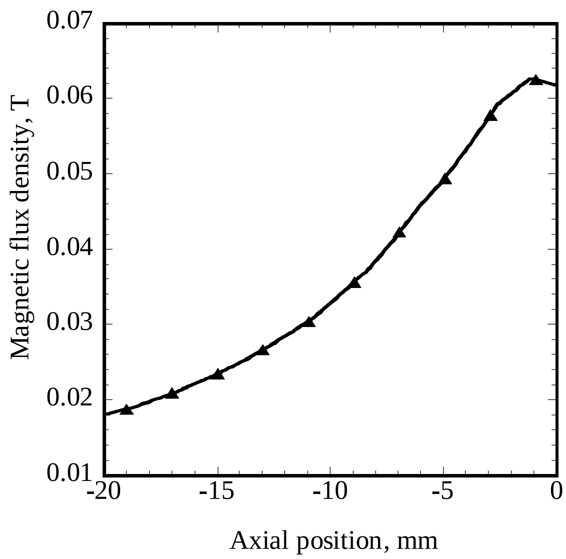

Fig. 2 Magnetic flux density profile.

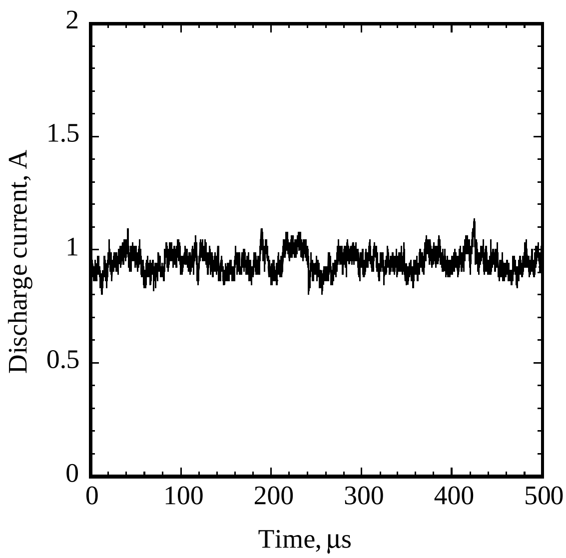

Fig. 3 Discharge current trace of a hollow cathode.

3. Oscillation Model

Several studies indicated that the oscillation was caused by ionization instability.[1-3] In addition, the electron mobility is the key role on this oscillation.[4] The set of equations describing the oscillation are below. The equation of continuity for neutral atom

$$\frac{\partial N_n}{\partial t} + \nabla(N_n V_n) = -\gamma N_n N_e \tag{1}$$

The equation of continuity for electron

$$\frac{\partial N_e}{\partial t} + \nabla(N_e V_e) = \gamma N_n N_e \tag{2}$$

Integrating Eqs. (2) and (3) over the whole ionization zone, they can be rewritten as follows.

$$\begin{aligned} &\int_V \frac{\partial N_n}{\partial t} dV + \int_S N_n V_n dS = \int_V -\gamma N_n N_e dV \\ &\int_V \frac{\partial N_e}{\partial t} dV + \int_S N_e V_e dS = \int_V \gamma N_n N_e dV \end{aligned} \tag{3}$$

These equations were solved analytically. Each parameter is assumed to consist of a steady state part and a small disturbance part that is proportional to $\exp[-i(\omega t - k z)]$. The wave number of k at plasma disturbance could be ignored since the relaxation time of plasma is less than oscillation period Each parameter is rewritten as below

$$\begin{aligned} N_e &= N_e + n_e \exp[-i\omega t] \\ N_n &= N_n + n_n \exp[-i(\omega t - k_n z)] \end{aligned} \tag{4}$$

For the simplicity, γ, N_n, N_e is considered as $\bar{\gamma}, \overline{N}_n, \overline{N}_e$

$$\bar{\gamma} = \frac{1}{L}\int_0^L \gamma\, dz, \quad \overline{N}_n = \frac{1}{L}\int_0^L N_n\, dz, \quad \overline{N}_e = \frac{1}{L}\int_0^L N_e\, dz \tag{5}$$

Substituting Eq. (4) into Eq. (3), the dispersion relation is written as,

$$\begin{aligned} &\omega^2 + \left\{ -i\bar{\gamma}\overline{N}_n + i\frac{V_{e\_exit} - r_S V_{e\_anode}}{L} + i\bar{\gamma}\overline{N}_e - GV_n \right\}\omega + iGV_n\left(\gamma\overline{N}_n - \frac{V_{e\_exit} - r_S V_{e\_anode}}{L} \right) \\ &- \bar{\gamma}\overline{N}_e \frac{V_{e\_exit} - r_S V_{e\_anode}}{L} = 0 \end{aligned} \tag{6}$$

where $G = \frac{k_n \times \exp[ik_n L]}{\exp[ik_n L] - 1}$, $\quad r_S = \frac{S_{anode}}{S_{exit}} = 1$

The stability condition of this oscillation Im [ω]<0 is written as,

$$b > 0 \tag{7}$$

$$b^2 c - abd + d^2 < 0 \tag{8}$$

where

$$a = -\mathrm{Re}[G] \times V_n$$

$$b = \frac{V_{e\_exit} - r_S V_{e\_anode}}{L} - \bar{\gamma}\overline{N}_n + \bar{\gamma}\overline{N}_e - \mathrm{Im}[G] \times V_n$$

$$c = -\mathrm{Im}[G] \times \left(\bar{\gamma}\overline{N}_n V_n - \frac{V_{e\_exit} - r_S V_{e\_anode}}{L} V_n \right) - \bar{\gamma}\overline{N}_e \frac{V_{e\_exit} - r_S V_{e\_anode}}{L}$$

$$d = \mathrm{Re}[G] \times \left(\bar{\gamma}\overline{N}_n V_n - \frac{V_{e\_exit} - r_S V_{e\_anode}}{L} V_n \right)$$

Equations (9) and (10) have to be rewritten about operation parameter in order to compare this model with the experimental results. Phase velocity in neutral atoms perturbation is assumed as their axial velocity.

$$k_n = C_n + i\,1/\lambda_{ne} \tag{9}$$

where, $C_n \approx \mathrm{Re}[\omega]/V_n$

Neutral particles temperature is estimated as 700K, therefore the neutral atom velocity is constant as

$$V_n = \frac{1}{4}\sqrt{\frac{8k_b T}{\pi M}} = 84 m/s \tag{10}$$

We estimate electron temperature from the electron energy balance equation as shown below.

$$\frac{5}{2}\nabla(kT_e n_e v_e) = en_e v_e \frac{d\phi}{dz} - \left\{(1+\beta)\varepsilon + \alpha\left(\frac{2}{1-\delta} + \frac{1-2\delta}{1-\delta}\chi\right)kT_e\right\}\gamma\, n_n\, n_e \tag{11}$$

where $\chi = \ln(1-\delta)\left(\frac{e^{0.5}}{4}\sqrt{\frac{8m_i}{\pi m_e}}\right)$

Ionization potential is 12.13eV for Xenon, and α, β, δ is chosen as 0.4, 2.0, 0.6, respectively according to Ref. 5. The electron density is estimated as below

$$\begin{cases} \overline{N}_e \approx N_{i\_exit} = \eta_u \dfrac{\dot{m}}{MSV_{i\_exit}} \\ \eta_u = 1 - Exp(-\dfrac{(1-\alpha)\, L \bar{\gamma}\, \overline{N}_e}{V_n}) \end{cases} \tag{12}$$

Ionization zone length L was estimated from the equation of continuity.

$$L = \frac{N_{i\_exit} V_{i\_exit} - 0}{\bar{\gamma}\, \overline{\mathrm{N}}_{\mathrm{n}} \overline{\mathrm{N}}_{\mathrm{e}} (1-\alpha)} = \frac{\eta_u \dot{m}}{\mathrm{eS}\, \bar{\gamma}\, \overline{\mathrm{N}}_{\mathrm{n}} \overline{\mathrm{N}}_{\mathrm{e}} (1-\alpha)} \tag{13}$$

Electron would move to anode with Bohm diffusion.

$$V_e = -\mu_\perp E - D_\perp \frac{\nabla N_e}{N_e} = -\mu(E + \frac{kT_e}{e}\frac{\nabla N_e}{N_e}) = -\frac{1}{16B}(E + \frac{kT_e}{e}\frac{\nabla N_e}{N_e}) \tag{14}$$

In case of Anode layer type, this model needs some changes. First, Electron moves to anode with classical diffusion.[4] An electron velocity is assumed to oscillate since the electron velocity is proportional to neutral atom density. Thus, electron velocity is written as below

$$V_e = V_e + v_e = -\frac{m_e < \sigma v >_{en}}{eB^2}(E + \frac{kT_e}{e}\frac{\nabla N_e}{N_e})(N_n + n_n) \equiv f(z)\,(N_n + n_n) \tag{15}$$

The dispersion relation in an Anode layer type is written as,

$$\begin{aligned} &\omega^2 + \left\{ i\,\bar{\gamma}\left(\overline{N}_e - \overline{N}_n\right) + i\,\frac{V_{e\_exit} - r_S\, V_{e\_anode}}{L} - GV_n \right\}\omega \\ &+ iG\left(\bar{\gamma}\,\overline{N}_n V_n - \frac{V_{e\_exit} - r_S\, V_{e\_anode}}{L} V_n + \bar{\gamma}\,\overline{N}_n\, f_{exit} N_{e\_exit}\right) - \bar{\gamma}\,\overline{N}_e\, \frac{V_{e\_exit} - r_S\, V_{e\_anode}}{L} = 0 \end{aligned} \tag{16}$$

The heat loss into the wall is neglected. Since the discharge chamber wall is kept at cathode potential, only ions collide with the wall chamber. Electron temperature was estimated from the electron energy balance equation as shown below.

$$\frac{5}{2}\nabla(kT_e n_e v_e) = e\Gamma_e \frac{d\phi}{dz} - (1+\beta)\gamma\, n_n\, n_e \varepsilon \tag{17}$$

$\overline{\mathrm{N}}_{\mathrm{e}}$ is estimated as Eqs. (12). L is estimated as Eqs. (13). r_s is estimated as 1.1 since ionization zone will be extended into hollow anode.

The stability condition of this oscillation Im [ω]<0 is written as,

$$b_a > 0 \tag{18}$$

$$b_a{}^2 c_a - a_a b_a d_a + d_a{}^2 < 0 \tag{19}$$

where

$$a_a = -\mathrm{Re}[G] \times V_n$$

$$b_a = \frac{V_{e\_exit} - r_S V_{e\_anode}}{L} - \bar{\gamma}\,\overline{N}_n + \bar{\gamma}\,\overline{N}_e - \mathrm{Im}[G] \times V_n$$

$$c_a = -\mathrm{Im}[G] \times \left(\bar{\gamma}\,\overline{N}_n V_n - \frac{V_{e\_exit} - r_S\, V_{e\_anode}}{L} V_n + \gamma N_n\, f_{exit} N_{e\_exit}\right) - \bar{\gamma}\,\overline{N}_e\, \frac{V_{e\_exit} - r_S V_{e\_anode}}{L}$$

$$d_a = \mathrm{Re}[G] \times \left(\bar{\gamma}\,\overline{N}_n V_n - \frac{V_{e\_exit} - r_S\, V_{e\_anode}}{L} V_n + \gamma N_n\, f_{exit} N_{e\_exit}\right)$$

4. Results and Discussion

To evaluate the oscillation depth of the experimental results, the amplitude of oscillation is defined as,

$$\Delta = \frac{R.M.S}{\overline{I_d}} = \frac{1}{\overline{I_d}}\sqrt{\frac{\int_0^{\tau}(I_d - \overline{I_d})^2}{\tau}}, \quad (\overline{I_d} = \frac{\int_0^{\tau} I_d}{\tau}) \tag{20}$$

Figure 4 shows the measured oscillation amplitude and stable/unstable operation condition deduced from theory. The hatched area indicates operational condition with no oscillation deduced from this theory. The stable operation zone deduced from this theory agreed with the experimental results in tendency. The difference might be due to the approximation during integration. However, this model would be a good expression of this oscillation mechanism.

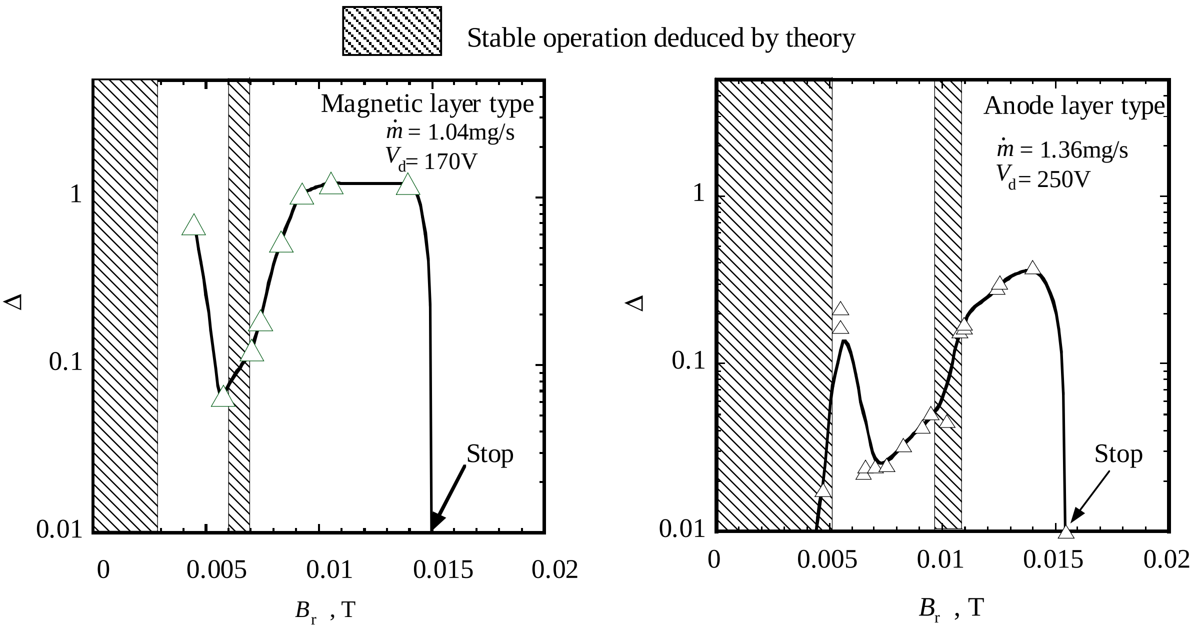

(a) (b)

Fig. 4 Stable/unstable operational condition.
(a)magnetic layer type $\dot{m}$ =1.04mg/s, V_d=170V (b) anode layer type $\dot{m}$ =1.36mg/s, V_d=250V

Examining this model, the criteria of Eq. (19) are almost covered that of Eq. (18). Therefore the criteria from equations (18) was examined. Due to this model, the left hand of equation (18) can be rewritten as

$$S_{anode}\left|V_{e\_anode}\right| - S\left|V_{e\_exit}\right| - \bar{\gamma}\,\overline{N}_n SL > 0 \tag{21}$$

Thus, in anode layer type, one of the attempts to depress the oscillation is increase in propellant utilization. Since in anode layer type, electrons move to anode with classical diffusion, electron velocity is proportional to neutral atom density. In addition, Eq. (21) shows that increase in S_a/S will make operation stable.

To confirm this, oscillation amplitude was measured for various anode width and anode position. *D* denotes the width of hollow and Z does the axial position of the anode tip measured from the exit of a guard ring as shown in Fig.5. With the increase in *Z*, stable operation range will be extended since *Z* will affect the *L* at the maximum. In addition, with the increase in *D*, stable operation range will be extended. Since the S_a will increase due to the extension of ionization zone into the hollow anode[7].

Table 1 shows the results for various anodes. The operation range of *B* with no oscillation was extended as above: that is, the stable operation range was wide with long acceleration channel ($Z \geq 3$), though there was no stable operation with the short acceleration channel ($Z \leq 2$). The stable operation range with large anode width ($D \geq 2$) was larger than that with narrow anode width (*D*=1). In addition, there was no stable operation if ϕ 1mm×36 holes anode was used instead of hollow anode.

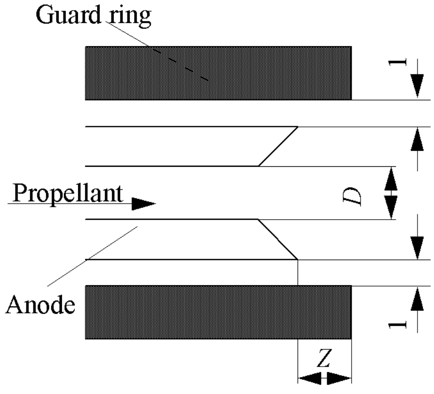

Fig.5 Schematic of acceleration zone

Table 1 Stable operational condition B_r , mT

D \ *Z*	1mm	2mm	3mm	4mm
1mm	Not available	Not available	7～10	7～8
2mm	Not available	Not available	≦5 7～10	≦4, 6～9, 13～14
3mm	Not available	≦7	≦5 6～10	≦4, 7～10

5. Conclusion

An ionization oscillation model considering electron dynamics was proposed. The deduced unstable operational condition agreed qualitatively with the experimental results. This model proposed that anode configuration will affect stability, and experimental results supported this assumption.

References

[1] Baranov V. I., Nazarenko Yu. S., Petrosov V. A., Vasin A. I., and Yashonov Yu. M. “Theory of oscillations and Conductivity For Hall Thruster” AIAA 96-3192, 32nd AIAA/ASME/SAE/ASEE joint Propulsion Conference, Lake Buena Vista, FL, July 1996

[2] Fife, J. M., Martinez-Sanchez, Manuel, and Azabo, James ”A numerical study of low-frequency discharge oscillations in Hall thrusters” AIAA96-3052, 33rd AIAA/ASME/SAE/ASEE joint Propulsion Conference. Seattle, WA, July, 1997

[3] Darnon F., Kadlec-Philippe C., Bouchoule A., and Lyszuk M. “Dynamic Plasma & Plume Behavior of SPT thrusters” AIAA98-3644, 34th AIAA/ASME/SAE/ASEE joint Propulsion Conference, July 1998, Cleveland, OH

[4] Yamamoto N., Nakagawa T., Komurasaki K. and Arakawa Y. “Discharge plasma Fluctuations in Hall Thrusters” Vacuum, vol.65, issues 3-4, 2002, pp. 375-381

[5] Smirnov V. A., “Electron Energy Balance in a Hall-Current Accelerator with an Extended Acceleration zone” Soviet Journal of Plasma Physics, Vol. 5, No.2,1979, pp.202-205.

[6] Kumakura K., Yasui S., Komurasaki K. and Arakawa Y. “Plasma Modeling of a Hollow Anode for an Anode Layer Type Hall Thruster” IEPC2003-116, 28th International Electric Propulsion Conference, Toulouse, France, March, 2003